than γ_1 by 30% (eq 24) so a fairly large difference might be expected on the basis of the above argument. However, Table I shows a 3.3% difference between $S_0(1)$ and $S(1)$ and only a 0.6% difference between $r_0(1)$ and $r(1)$. The explanation of this paradox most likely has to do with the fact that the *amplitude* of the shorter modes is small compared to the longer ones according to eq 34. On the nanosecond time scale, the shorter modes do make a contribution to fluorescence depolarization but they are overwhelmed by the larger amplitude contributions of longer modes. The behavior in the $t = 0$ limit of $dS(t)/dt$ also supports this. The *initial* decay rate is dominated by the shortest modes but because of their low amplitude, they contribute little to the net decay.

V. Conclusions

Even though the response $\tau(z)$ depends rigorously on the state (given by $\dot{\phi}(z)$) of the entire cylinder, it is determined locally in practice. Modeling DNA as a continuous elastic cylinder, $\tau(z)$ at some position is determined primarily by the $\dot{\phi}$'s of the 11 nearest-neighbor base pairs on either side of the one in question. This in itself cannot be taken as justification for using the Perrin result (eq 5) to accurately account for torsional hydrodynamic interaction since it is valid only if the local gradient in $\dot{\phi}$ along the cylinder is small. In terms of normal coordinates, the gradient in $\dot{\phi}$ is small provided the amplitudes of the long-wavelength normal modes are collectively large compared to those of the short-wavelength normal modes.

In experiments like fluorescence depolarization,[2-6,8,9] EPR,[7] depolarized light scattering,[10] and NMR[11-13] the measurements are related to time autocorrelation functions of the form $\langle e^{ik(\phi(t)-\phi(0))} \rangle$ ($k = 1, 2$). From eq 34-37, it can thus be seen that these experiments monitor the decay of torsion normal modes weighted by their thermal equilibrium amplitudes. Since the short modes have small amplitudes, the above experiments are dominated by the long-wavelength modes, which means replacing γ_l with eq 5 is justified. It should be emphasized, however, that this justification is a consequence of the limited resolution of the experiments. Although these conclusions were arrived at by considering the particular case of DNA, they would also be true for long, stiff, wormlike chains in general.

Acknowledgment. The author thanks Professor John Schellman for encouragement and support. Thanks are also due to Professor Jeff Skolnick for helpful input into this problem. This research was funded in part by grants from the U.S. Public Health Service (Grant GM 20195) and the National Science Foundation (Grant PCM 8104339) (both to J.A.S.) and by Fellowship No. 1 F32 GM 08090-01 from the National Institutes of Health.

References and Notes

(1) Allison, S. *Macromolecules* **1982**, *15*, 1544.
(2) Perrin, F. *J. Phys. Rad.* **1934**, *5*, 497; **1936**, *7*, 1.
(3) Wahl, Ph.; Paoletti, J.; LePecq, J. B. *Proc. Natl. Acad. Sci. U.S.A.* **1970**, *65*, 417.
(4) Thomas, J. C.; Allison, S.; Appellof, C.; Schurr, J. M. *Biophys. Chem.* **1980**, *12*, 177.
(5) Schurr, J. M.; Shibata, J.; Allison, S.; Thomas, J. C. *Biophys. J.* **1981**, *33*, 317a.
(6) Millar, D.; Robbins, R.; Zewail, A. *Proc. Natl. Acad. Sci. U.S.A.* **1980**, *77*, 5593.
(7) Robinson, B.; Forgacs, G.; Dalton, L.; Frisch, H. *J. Chem. Phys.* **1980**, *73*, 4688.
(8) Barkley, M.; Zimm, B. *J. Chem. Phys.* **1979**, *70*, 2991.
(9) Allison, S.; Schurr, J. M. *Chem. Phys.* **1979**, *41*, 35.
(10) Carpenter, D.; Skolnick, J. *Macromolecules* **1981**, *14*, 1284.
(11) Allison, S.; Shibata, J.; Wilcoxon, J.; Schurr, J. M. *Biopolymers* **1982**, *21*, 729.
(12) Hogan, M.; Jardetzky, O. *Proc. Natl. Acad. Sci. U.S.A.* **1979**, *76*, 6341.
(13) Hogan, M.; Jardetzky, O. *Biochemistry* **1980**, *19*, 3460.
(14) Merzbacher, E. "Quantum Mechanics"; Wiley: New York, 1970.
(15) "Handbook of Mathematical Functions"; Abramowitz, M., Stegun, I., Eds.; U.S. Government Printing Office: Washington, D.C., 1972; NBS Applied Math Series No. 55.
(16) Rizzo, V.; Schellman, J. *Biopolymers* **1981**, *20*, 2143.
(17) Kam, Z.; Borochov, N.; Eisenberg, H. *Biopolymers* **1981**, *20*, 2671.
(18) Hagerman, P. *Biopolymers* **1981**, *20*, 1503.
(19) Elias, J. G.; Eden, D. *Macromolecules* **1981**, *14*, 410.
(20) Cairney, K.; Harrington, R. *Biopolymers* **1982**, *21*, 923.
(21) Zimm, B. *J. Chem. Phys.* **1956**, *24*, 269.
(22) Lin, S.-C.; Schurr, J. M. *Biopolymers* **1978**, *17*, 425.
(23) Hogan, M.; Dattagupta, N.; Crothers, D. *Biochemistry* **1979**, *18*, 280.

Particle Scattering Factor of Polymer Chains with Excluded Volumes

Ichiro Noda,* Masanori Imai, Toshiaki Kitano,[1] and Mitsuru Nagasawa

Department of Synthetic Chemistry, Nagoya University, Furo-cho, Chikusa-ku, Nagoya, Japan 464. *Received February 8, 1982*

ABSTRACT: Particle scattering factors of polystyrenes having high molecular weights and narrow molecular weight distributions in light scattering were experimentally determined for comparison with the theories so far published. None of the theories satisfactorily agree with experiments over a wide range of scattering angle. An empirical equation is presented.

Introduction

The particle scattering factor, $P(\theta)$, for Gaussian chains in light scattering was calculated by Debye[2] to be

$$P(\theta) = 2u^{-2}[\exp(-u) - 1 + u] \quad (1)$$

where $u = q^2\langle s^2 \rangle$, $q = 4\pi/\lambda \sin(\theta/2)$, $\langle s^2 \rangle$ is the mean square radius of gyration of the polymer, λ is the wavelength of the incident light in the solution, and q is the magnitude of the wave vector. It has been confirmed that $P(\theta)$ for nonionic polymers[3] and $P(\theta)$ for polyelectrolytes[4,5] in Θ solvents agree well with eq 1 if the samples have sharp molecular weight distributions.

As the thermodynamic interaction between segments increases or as the solvent becomes better, polymer chains expand and become non-Gaussian on account of the excluded volume effect. Theoretical calculations of $P(\theta)$ for non-Gaussian chains were presented by Peterlin[6] and integration forms by Ptitsyn[7] and Benoit.[8] They introduced

0024-9297/83/2216-0425$01.50/0

a parameter ϵ to express the non-Gaussian character of the chain due to the excluded volume effect, writing

$$\langle r_{ij}^2 \rangle \propto |i - j|^{1+\epsilon} \quad (2)$$

where $\langle r_{ij}^2 \rangle$ is the mean square distance between the ith and jth segments. Substituting eq 2 into the segment distribution function of a Gaussian form, they obtained

$$P(\theta) = \int_0^1 2(1 - x) \exp(-ux^{1+\epsilon})\, dx \quad (3)$$

where

$$u = \frac{(2 + \epsilon)(3 + \epsilon)}{6} q^2 \langle s^2 \rangle$$

If $\epsilon = 0$, eq 3 reduces to the Debye function, eq 1. The approximate estimation of ϵ is possible from the molecular weight dependence of the radius of gyration.

$$\langle s^2 \rangle \propto M^{1+\epsilon} \quad (4)$$

If the excluded volume effect theory of the α^5 type is applicable, ϵ in very good solvents is approximately 0.2.

Recently, Farnoux et al.[9] presented a theory based on the so-called "blob" model, in which the distribution of segments is Gaussian up to a critical segment number N_c and is discontinuously changed to the non-Gaussian one of Peterlin's type ($\epsilon = 0.2$) beyond that segment number. In this theory, $P(\theta)$ is given by

$$P(\theta) = \frac{2Z}{Y^2}\{Y - Z + e^{-Y}[Z(1 + Y) - Y]\} + \frac{1}{\nu X^{1/2\nu}}\left[\gamma\left(\frac{1}{2\nu}, X\right) - \gamma\left(\frac{1}{2\nu}, Y\right) - \frac{1}{X^{1/2\nu}}\left(\gamma\left(\frac{1}{\nu}, X\right) - \gamma\left(\frac{1}{\nu}, Y\right)\right)\right] \quad (5)$$

where $\nu = (1 + \epsilon)/2$, $X = q^2\langle s^2 \rangle$, $Z = N_c/N$, $Y = XZ^{2\nu}$, N is the total segment number in the polymer chain, and γ is the incomplete gamma function. If $Z = 1$, eq 5 reduces to eq 1, whereas if $Z = 0$ it reduces to eq 3. Moreover, the behavior of $P(\theta)$ in the crossover region was discussed in detail by Francois et al.[10]

In general, if the distribution function $W(r_{ij})$ is spherically symmetric and has a general scaling form such as

$$W(r_{ij}) \propto \frac{1}{\langle r_{ij}^2 \rangle^{3/2}} F(r_{ij}/\langle r_{ij}^2 \rangle^{1/2}) \quad (6)$$

the $P(\theta)$ function has the limiting form (7) irrespective of the functional form F at $q^2\langle s^2 \rangle \gg 1$.[11]

$$P(\theta) \propto q^{-1/\nu} \quad (7)$$

In previous papers,[4,5] it was reported that $P(\theta)$ of a polyelectrolyte, poly(sodium acrylates) having sharp molecular weight distributions, in the presence of an added salt agrees well with eq 3. On the other hand, $P(\theta)$ of nonionic polymers in good solvents does not satisfactorily agree with eq 3 and reasonable values of the radius of gyration are generally obtained by employing eq 1 in the range of low scattering angles.[3,12,13]

The purpose of this work is to observe the particle scattering factors of polystyrenes having high molecular weights and narrow molecular weight distributions and to compare the data with theoretical $P(\theta)$ equations.

Experimental Section

Samples. For the present purpose, it is necessary to use polymer samples having very high molecular weights and narrow molecular weight distributions. One of the polystyrene samples, μ-002, was prepared in previous work[14] and the other ones were provided by Toyo Soda Manufacturing Co. Their molecular characteristics are shown in Table I. Toluene, used as a good solvent for polystyrenes, was purified by the same method described in a previous paper.[3]

Table I
Light Scattering Data of Polystyrenes in Toluene at 25 °C

sample code	$M_w \times 10^{-6}$	$\langle s^2 \rangle \times 10^{10}$, cm^2	$A_2 \times 10^4$, cm^3 mol g^{-2}
F-850	8.4	2.4	1.6$_8$
μ-002	11	3.4$_6$	1.4$_9$
F-2000	21	7.0	1.2$_9$

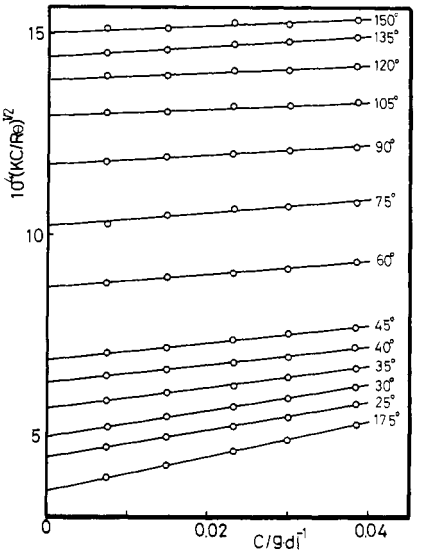

Figure 1. Square root plot of KC/R_θ against polymer concentration at various scattering angles. Sample, μ-002; solvent, toluene; temperature, 25 °C.

Light Scattering Measurements. A Fica 50 automatic light scattering photometer was used with 436-nm natural light. The scattering angle was in the range 15–150°. The calibration constant of the photometer was determined by measuring light scattered from benzene at 25 °C.

Great care was taken in preparation of the sample solutions to prevent degradation of the polymers. The optical purification of solutions for light scattering measurements was carried out by ultracentrifugation at about 50000g for about 2 h. All measurements were carried out at 25 °C. For the refractive index increment (dn/dC) of polystyrene in toluene, a value reported by Norberg and Sundelöf,[15] 0.1129 cm^3 g^{-1}, was employed.

Results and Discussion

The light scattering data from polymer solutions can be expressed by

$$(KC/R_\theta)_{\theta=0} = 1/M_w + 2A_2C + \ldots \quad (8)$$

$$(KC/R_\theta)_{C=0} = 1/[M_wP(\theta)] \quad (9)$$

where A_2 is the second virial coefficient and K is a well-known coefficient; $K = 2\pi^2 n_0^2 (dn/dC)^2/N_A\lambda_0^4$. Therefore, $P(\theta)$ can be obtained from

$$P^{-1}(\theta) = (KC/R_\theta)_{C=0}M_w = (KC/R_\theta)_{C=0}/(KC/R_\theta)_{C=0,\theta=0} \quad (10)$$

To make the extrapolation to zero polymer concentration easier, a square root plot was employed as shown in Figure 1.

In order to compare the experimental values of $P(\theta)$ with theories, it is necessary to know the mean square radius of gyration $\langle s^2 \rangle$ of the polymer. The reciprocal of $P(\theta)$ can be expanded in terms of $\sin^2(\theta/2)$ without any assumption regarding the conformation of the polymers:

$$P^{-1}(\theta) = 1 + (16\pi^2/3\lambda^2)\langle s^2 \rangle \sin^2(\theta/2) + \ldots \quad (11)$$

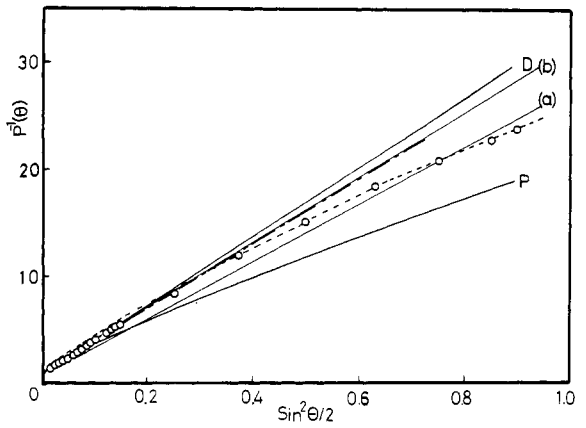

Figure 2. Comparison of experimental $P(\theta)$ of polystyrene with various theories. Sample, μ-002; $\langle s^2 \rangle = 3.46 \times 10^{-10}$ cm^2. The dash-dot line shows the initial slope. The solid lines D and P show calculated values of eq 1 and 3, respectively. The thin solid lines show the calculated values of eq 5, assuming $Z = 0.4$ (a) and $Z = 0.8$ (b). The broken line shows the calculated values of eq 3, assuming $\epsilon = 0.2$ and $\langle s^2 \rangle = 5.63 \times 10^{-10}$ cm^2.

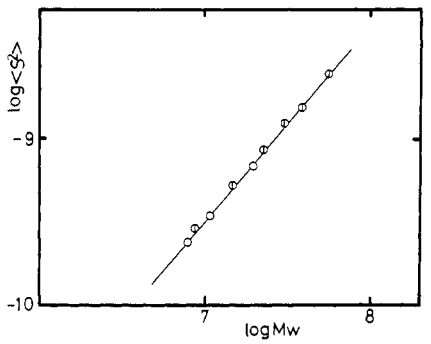

Figure 3. Molecular weight dependence of $\langle s^2 \rangle$ of polystyrene in toluene (○) and benzene (⊕)[16] at 25 °C.

Figure 2 shows an example of $P^{-1}(\theta)$ vs. $\sin^2(\theta/2)$ for polystyrenes in toluene. The initial slopes were graphically determined on the figures. The graphical determination of the initial slopes is surely somewhat ambiguous, but the ambiguity is not so great as to affect the following discussion. The values of $\langle s^2 \rangle$ calculated from the initial slopes are shown in Table I. The values of the second virial coefficient A_2 were also determined by the ordinary procedure and are listed in Table I.

The values of $\langle s^2 \rangle$ in Table I are double-logarithmically plotted against molecular weight together with the data in the literature[16] in Figure 3. The slope gives $\epsilon = 0.2$. The experimental values of $P(\theta)$ of three samples, moreover, are replotted in the form of eq 7 in Figure 4A. From the slopes at high q, we have $\epsilon = 0.2$. These results are in agreement with the excluded volume effect theory of the α^5 type. Thus, we assume $\epsilon = 0.2$ in the following discussion.

If we plot the $P(\theta)$ data of the three samples in terms of $q^2\langle s^2 \rangle$, we have Figure 5. The calculated values of eq 1 and 3 using $\epsilon = 0.2$ are shown by the solid lines D and P, respectively, for comparison with experimental data in Figures 2 and 5. Both figures show that the experimental $P(\theta)$ of polystyrene in good solvents cannot fully be explained either by eq 1 or by eq 3. Even if we change ϵ, it is not possible to fit the theoretical line of eq 3 with experimental data in a satifactorily wide range of scattering angle. The calculated values of eq 5, using Z as a parameter, are also shown by thin solid lines in Figure 2. It is clear that the blob model cannot improve the agreement between theory and experiments. Moreover, if we plot the

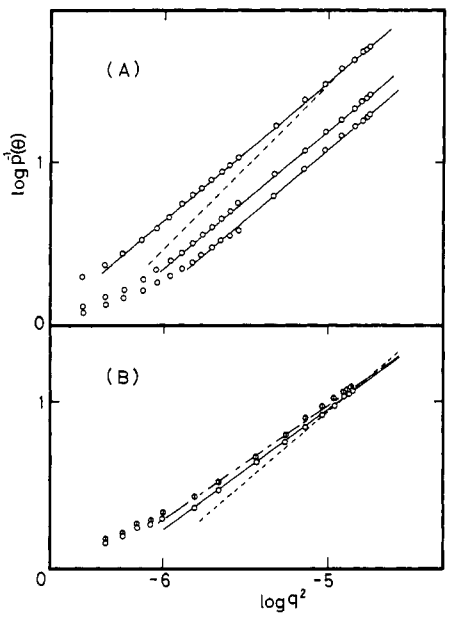

Figure 4. Double-logarithmic plots of $P^{-1}(\theta)$ vs. q^2. (A) Polystyrene in toluene. The samples are F-2000, μ-002, and F-850 from top to bottom. The slopes of the solid and broken lines are $^5/_6$ ($\nu = 0.6$) and 1 ($\nu = 0.5$), respectively. (B) Poly(sodium acrylate) in NaBr solutions. Degree of neutralization, 0.6; NaBr concentration, 0.025 (○) and 0.01 M (⊕). The slopes of the straight lines are 1/1.24 ($\nu = 0.62$) for the solid line, 1/1.32 ($\nu = 0.66$) for the dash-dot line, and $^5/_6$ ($\nu = 0.6$) for the broken line.

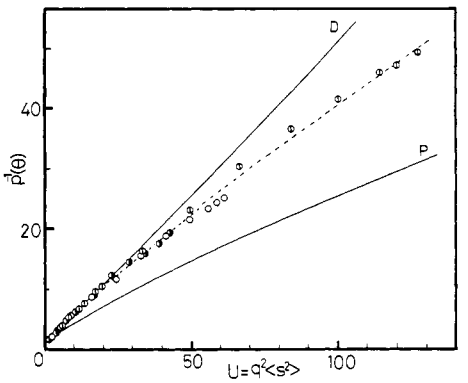

Figure 5. Experimental $P^{-1}(\theta)$ of three samples plotted against $q^2\langle s^2 \rangle$. The circles (◑), (○), and (⊕)denote data for F-850, μ-002, and F-2000, respectively. The solid lines D and P are the same as in Figure 2. The broken line shows the calculated values of eq 12, assuming $Z = 0.05$.

calculated values of eq 5 in the form of log $P^{-1}(\theta)$ vs. log q^2, the slope at high q gives $\nu = 0.5$ ($\epsilon = 0$), as shown by the broken line in Figure 4A.

Two features can be pointed out in the comparison between the theories and experimental data in Figure 2 and 5. In the low q range, the experimental $P(\theta)$ agrees with the Debye function (1). This is in accord with our experience that the radius of gyration of nonionic polymers can more reasonably be determined by employing the equation of Debye than by employing that of Peterlin et al.[3,12,13] On the other hand, if we observe the high q range only, i.e., if we fit eq 3 with the experimental data only at high scattering angles, assuming that $\epsilon = 0.2$ but $\langle s^2 \rangle$ is variable, we have satisfactory agreement between the calculated and experimental values, as shown by the broken line in Figure 2. This result is consistent with the data in Figure 4A.

These features suggest that the particle scattering factor of an isolated linear polymer in a good solvent can be expressed by the equation

$$P(\theta) = \frac{2}{X}\left[e^{-ZX}(1 - Z) - \frac{1}{X}(e^{-ZX} - e^{-X}) \right] + \frac{Z}{\nu Y^{1/2\nu}}\left[\gamma\left(\frac{1}{2\nu}, Y\right) - \frac{Z}{Y^{1/2\nu}}\gamma\left(\frac{1}{\nu}, Y\right) \right] \quad (12)$$

where X and γ have the same definitions as in eq 5 but Z is an adjustable parameter between 1 and 0 and $Y = ZX$. This equation agrees with eq 1 if $Z = 0$ and with eq 3 if $Z = 1$. At an intermediate value of Z, eq 12 describes the Debye function form (eq 1) in the low q range and the Peterlin function form (eq 3) in the high q range. Equation 12 happens to be the same as eq 3.8 of ref 9 in the blob theory for a polymer chain in semidilute solutions. However, their physical meanings are different; $\langle s^2 \rangle$ is expected to increase in proportion to N in semidilute solutions, whereas the experimental values, which are proportional to $N^{1+\epsilon}$, are inserted into $\langle s^2 \rangle$ for an isolated polymer in good solvents.

Assuming that Z is an adjustable parameter and $\nu = 0.6$, we evaluated $P(\theta)$ from eq 12 and compared them with experimental data. As shown in Figure 5, satisfactory agreement between the calculated and experimental values is obtained if we assume $Z = 0.05$.

As explained in the Introduction, $P(\theta)$ of poly(sodium acrylate), on the other hand, in the presence of an added salt agrees with eq 3 over the entire range of q. This means that $Z = 1$ in eq 12 for polyelectrolytes. Although the interaction between nonionic segments and the electrostatic interaction between charged groups are both considered to be excluded volume effects, the former may drop much more rapidly than the latter. Moreover, the same data are replotted in the form of eq 7 in Figure 4B. The slopes at high q can give values higher than 0.6 for ν, i.e., higher than 0.2 for ϵ, at low ionic strengths.

Finally, it is to be noted that the interpenetration function $\Psi(\bar{z})$ ($=A_2M^2/4\pi^{3/2}N_A\langle s^2 \rangle^{3/2}$) calculated from the data in Table I is found to be 0.24, 0.21, and 0.23 for $M = 0.84 \times 10^7$, 1.1×10^7 and 2.1×10^7, respectively. This result agrees with our previous conclusion that $\Psi(\bar{z})$ converges to 0.2_1 as the molecular weight increases[3,17] and also with the data reported later.[16,18]

Acknowledgment. We thank the Ministry of Education, Science and Culture, Japan, for financial support through a Grant-in-Aid for Scientific Research (Grant 347079).

Registry No. Polystyrene, 9003-53-6.

References and Notes

(1) School of Material Science, Toyohashi University of Technology, Tempaku-cho, Toyohashi, Japan 440.
(2) Debye, P. J. *Phys. Colloid Chem.* **1947**, *51*, 18.
(3) Kato, T.; Miyaso, K.; Noda, I.; Fujimoto, T.; Nagasawa, M. *Macromolecules* **1970**, *3*, 777.
(4) Kitano, T.; Taguchi, A.; Noda, I.; Nagasawa, M. *Macromolecules* **1980**, *13*, 57.
(5) Nagasawa, M.; Noda, I.; Kitano, T. *Biophys. Chem.* **1980**, *11*, 435.
(6) Peterlin, A. *J. Chem. Phys.* **1955**, *23*, 2464.
(7) Ptitsyn, O. B. *Zh. Fiz. Khim.* **1957**, *31*, 1091.
(8) Benoit, H.; *C. R. Hebd. Seances Acad. Sci.* **1957**, *245*, 2244.
(9) Farnoux, B.; Boue, F.; Cotton, J. P.; Daoud, M.; Jannink, G.; Nierlich, M.; de Gennes, P.-G. *J. Phys. (Paris)* **1978**, *39*, 77.
(10) Francois, J.; Schwartz, T.; Weill, G. *Macromolecules* **1980**, *13*, 564.
(11) Mazur, J.; McIntyre, D. *Macromolecules* **1975**, *8*, 464.
(12) Smith, T. E.; Carpenter, D. K. *Macromolecules* **1968**, *1*, 204.
(13) Fujita, H. *Polym. J.* **1970**, *1*, 537.
(14) Fujimoto, T.; Nagasawa, M. *Polym. J.* **1975**, *7*, 397.
(15) Norberg, P. N.; Sundelöf, L. O. *Makromol. Chem.* **1964**, *77*, 77.
(16) Miyaki, Y.; Einaga, Y.; Fujita, H. *Macromolecules* **1980**, *11*, 1180.
(17) Noda, I.; Kitano, T.; Nagasawa, M. *J. Polym. Sci., Polym. Phys. Ed.* **1977**, *15*, 1129.
(18) Fukuda, M.; Fukutomi, M.; Kato, Y.; Hashimoto, T. *J. Polym. Sci., Polym. Phys. Ed.* **1974**, *12*, 871.

Small-Angle X-ray Scattering Study of Density Fluctuation in Polystyrene Annealed below the Glass Transition Temperature

Ryong-Joon Roe* and J. J. Curro

Department of Materials Science and Metallurgical Engineering, University of Cincinnati, Cincinnati, Ohio 45221. *Received July 12, 1982*

ABSTRACT: The intensity of X-rays scattered at small angles provides a measure of the density fluctuation in amorphous solids. Above T_g the density fluctuation is thermally induced and proportional to compressibility, while below T_g it has in addition a contribution from frozen-in inhomogeneities. When polystyrene was annealed below T_g, the observed behavior depended on the annealing temperature. Between 80 and 100 °C the density fluctuation decreased approximately linearly with the logarithm of time, while below 80 °C it remained constant in the 24-h observation period. On constant-rate cooling, the observed density fluctuation against temperature could be represented by three linear sections, the liquid line above T_g, the glass line below about 80 °C, and a transition line between about 80 and 100 °C. Three narrow fractions of 17 500, 220 000, and 1 800 000 molecular weight and a commercial sample were studied and were observed to give a density fluctuation in glass that depended sensitively on molecular weight. The behavior of the density fluctuation on isothermal annealing, on constant-rate cooling, and on changing molecular weight is very different from the behavior of specific volume under similar conditions. Whereas the specific volume might provide a measure of the average free volume content, the density fluctuation can be interpreted to reveal the distribution of free volume. The small-angle X-ray scattering measurement thus offers a glimpse into the structure of glass from a very different angle of view and would prove a valuable tool in our efforts to understand the nature of glass.

I. Introduction

When a glassy material is annealed at temperatures moderately below its glass transition temperature, its internal structure undergoes a slow relaxation toward equilibrium. This structural relaxation can be demonstrated through measurements of various properties, for example, specific volume,[1] heat content,[2] and creep properties.[3] Each of these properties provides a "window"

0024-9297/83/2216-0428$01.50/0